Caving 2026 – A van As, D Cumming-Potvin & J Wesseloo (eds)

doi:10.36487/ACG_repo/2645_40

Caveability evaluation of block caving and prediction of caving fragmentation for a gold mine

Ji Youtong [a], Xie Lianku [b], Liang Zhonghao [a], Cao Hui [a,*], Zhang Guang [b], Wang Aiai [a], Ou Shengqing [a], Liu Peng [b]

[a] *College of Resources and Safety Engineering, University of Science and Technology Beijing, China*

[b] *Information Research Institute of Ministry of Emergency Management, China*

Abstract

Block caving is a mining approach characterised by large production scale, low mining costs, and high production efficiency, making it one of the important choices for large-scale underground mine exploitation in China. This paper focuses on the block caving mining plan selected in the open pit to underground transition production planning design of a gold mine. By comprehensively utilising methods such as machine learning, big data analysis, 3D modelling, and numerical analysis, a systematic study on the caveability and caving fragmentation characteristics of ore and rock in the deep area of the mining area is conducted. For the basic information required in the mining rock mass rating (MRMR) evaluation system, detailed core engineering geological logging and investigation analysis of structural surfaces in open pit slopes are carried out. The K-nearest neighbours algorithm is introduced to enhance the reliability of predicting engineering geological information in unknown areas, and then 3D modelling software is used to construct a 3D digital characterisation model of the engineering geological features of ore and rock based on multiple evaluation index systems, achieving refined classification evaluation of the caveability in the disturbed area. By comprehensively utilising the caving diagram method and caving fragmentation prediction analysis software, the prediction analysis of caving area and caving fragmentation is conducted, and combined with the mining design plan, the 3D numerical analysis method is used to simulate and study the caving characteristics of surrounding rock during the caving process of the mine, verifying the rationality of the caveability evaluation results. The research results show that the average MRMR of ore and rock within the 840 m to surface range of this gold mine is 54, with a caveability grade of class III moderate caving. The initial caving area of the eastern mine section is approximately 5,000 m², and the initial caving area of the western mine section is approximately 3,000 m². The predicted caving fragmentation of this gold mine is an average of 0.34–1.22 m³. The related results can provide a basic basis for the block caving mining design, optimisation of the bottom structure, and safe production of the mine.

Keywords: *block caving, MRMR, 3D visualisation, caveability, caving fragmentation, machine learning*

1 Introduction

Block caving is a mining method characterised by large production scale, low operating costs, and high efficiency (Wu et al. 2021; Wang et al. 2025). It has also become one of the important options for large-scale underground mining in China (Wang et al. 2023). As shallow resources gradually deplete, an increasing number of mines are transitioning from open pit to underground mining, where block caving demonstrates significant technical and economic advantages (Mariager & Fargher 2024). Caveability assessment and caving fragmentation prediction are fundamental to block caving design, directly influencing the feasibility demonstration of the mining method, the determination of undercutting strategies, and the stability of the extraction level structure (Liu & He 2024).

[*] Corresponding author. Email address: caohui_ustb@126.com

Considerable research has been conducted on caveability assessment and caving fragmentation prediction in block caving. In terms of caveability assessment, the caving chart method and the mining rock mass rating (MRMR) classification system proposed by Laubscher (1994) have become industry-standard approaches. Feng et al. (2008) conducted a caveability study of the Jinchuan III mining area using the Laubscher caving chart, calculating the initial and persistent caving hydraulic radii for each evaluation zone. Cao et al. (2016) established a three-dimensional caveability assessment model using the MRMR method, which was subsequently validated at the Don Javier mine. In recent years, machine learning techniques have been introduced into this field. Liu & He (2024) developed a caveability evaluation system incorporating fuzzy comprehensive assessment, while Wang et al. (2023) conducted a caveability assessment using both the Laubscher caving chart and three-dimensional numerical simulation. Regarding caving fragmentation prediction, Tong (2025) employed Monte Carlo simulation techniques and the block cave fragmentation (BCF) software to predict fragmentation in a porphyry copper mine, obtaining the distribution patterns of both primary and draw fragmentation. In terms of engineering applications, Zhang & Hocking (2022) discussed block cave design and planning in the context of the Carrapateena mine. Palabora Mining Company has successfully operated a world-class block cave mine, providing valuable experience for similar operations.

However, systematic research on caveability and caving fragmentation for large-scale block caving during the open pit to underground transition period remains relatively limited, particularly regarding the integrated application of refined assessment tools such as machine learning, three-dimensional modelling, and numerical simulation. This paper utilises the MRMR evaluation system proposed by Laubscher, and based on field surveys and drilling geological information, the K-nearest neighbours (KNN) nearest algorithm is introduced to predict drilling data in unknown areas and to construct an MRMR three-dimensional evaluation model, to achieve spatial visualisation analysis of collapse potential, thereby providing guidance for zone mining. The Laubscher diagram and BCF software are adopted to predict caving area and fragment size, while numerical simulation of undercutting and drawing verifies the caveability evaluation, providing scientific support for block caving mining.

2 Project overview

The mine is currently operated as an open pit operation. The mining area is situated on a plateau. The exposed strata in this area consists of the Jianshan, Halahot, and Bilute formations of the Baiyunebo Group within the Middle Proterozoic. The mineralisation of the deposit is located within the Bilute Formation of the Baiyunebo Group, and the orebody is strictly controlled by stratigraphic and tectonic fracture zones, as well as foliation zones. The mineralised zone is divided into eastern and western sections and exhibits an arc-shaped distribution. As shown in Figure 1, the mining area has well-developed structural fissures, displaying a variety of types that are relatively dense, which greatly affects the integrity of the rock mass in the mining area. Therefore, this mine is suitable for adopting the natural caving method as the mining method.

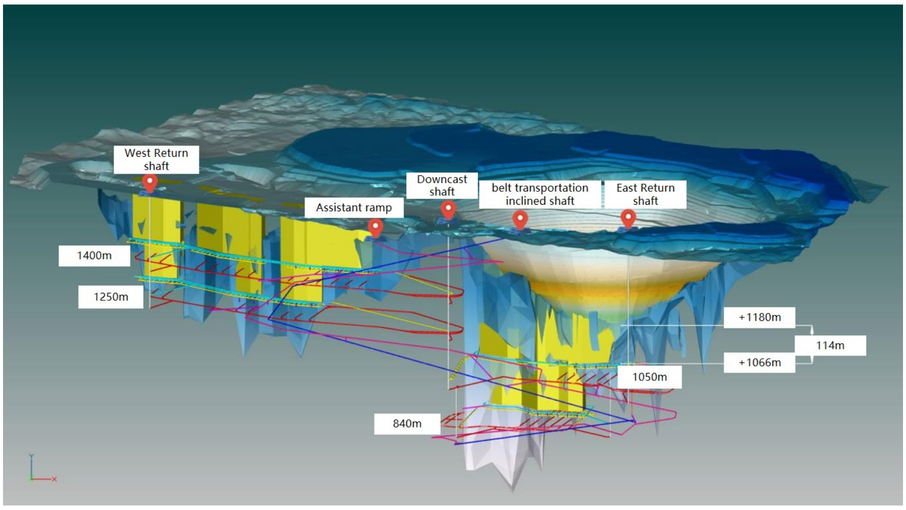

(a)

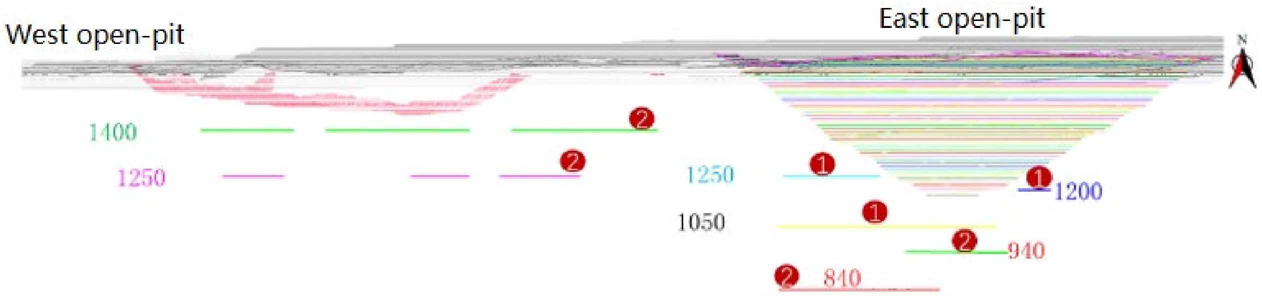

(b)

Figure 1 3D and section map of orebody distribution in mining area. (a) 3D map of orebody distribution; (b) Section map of orebody distribution

To accurately assess the rock mass stability of this mine, extensive rock mechanics research was conducted. Based on the existing conditions of the mining area, logging was carried out on 12 new boreholes and 92 existing boreholes, along with field fracture surveys of exposed rock surfaces, ultrasonic borehole imaging logging, and physical and mechanical testing of ore and rock. This yielded metrics such as rock quality designation (RQD) ratings, uniaxial compressive strength of the rock, strike and dip of structural planes (including dip angle and strike), surface roughness of structural planes, joint spacing, and joint density. These data provide a solid foundation for subsequent analysis of the ore and host rock's friability using MRMR statistical techniques. The specific scope of work is shown in Table 1.

Table 1 Detailed workload schedule

Job description	Work methods	Workload details
Geological survey of deep slopes	Photogrammetry and compass surveying	16 measurement points, 48 data sets
Survey of drillhole structures	Logging of existing drill cores	86 drill holes, 77,400 metres
Drilling survey	Ultrasonic imaging testing	13 drill holes, 10,530 metres
Rock sampling and mechanical testing	Uniaxial and triaxial compression tests, Brazilian split-tensile test	78 items
	Onsite point load testing	528 items
Soil stress testing	Hydraulic fracturing	2 drill holes, 23 tests

The study area for this rock stability analysis covers the eastern section of phase I from 1,050 m to the surface (outside the open pit boundary), as well as the eastern section of phase II from 840 to 1,050 m and the western section from 1,250 m to the surface.

3 Analysis and evaluation of Caveability

3.1 Mining rock mass rating statistical techniques

MRMR was proposed by DH Laubscher and J Jakubec in 2000 based on the original rock mass classification index in-situ rock mass rating (IRMR) , with its evaluation criteria shown in Table 2. The statistical analysis of the MRMR values for this gold mine will be based on the laboratory and field work of this gold mine, after rock block strength (RBS) scoring, joint spacing (JS) scoring, joint condition (JC) coring, and adjustments for groundwater influence, to conduct a statistical analysis of the ore rock MRMR.

Table 2 Evaluation criteria for the natural collapse method based on mining rock mass rating (Laubscher 1994)

Fracture resistance classification		V	IV	III	II	I
Mining rock mass rating		0–20	21–40	41–60	61–80	80–100
Fragility		Excellent	Good	Average	Poor	Very poor
Initial hydraulic radius (m)		1–8	8–18	18–32	32–50	>50
Particle size (m)		0.01–0.3	0.1–2.0	0.4–5	1.5–9	3–20
Explosive consumption for secondary blasting (g/t)		0–50	50–150	150–400	400–700	>700
Amount of waste rock mixed into the overburden (%)		0	15	30	45	>60
Drawzone diameter (m)		6–7	8–9	10–11.5	12–13.5	15
Distance between drawpoints (m)	Mineral extraction by raking	5–7	7–10	9– 12	—	—
	Loader unloading ore	9	9-13	11-15	13-18	—

3.2 Caveability estimation in partitions

According to the caveability evaluation criteria and MRMR statistical techniques, adopting a zoned evaluation approach can more intuitively and finely reveal the distribution of rock breakability in this mining area, enabling more targeted and safe rock breaking based on the statistical results of rock breakability at different stratifications. For the drilling database of this gold mine, based on the characteristics of orebody occurrence in the current study area, the MRMR values of rock in each stratification between the 840 m level to surface in the east mining section and the 1,250 m level to surface in the west mining section were statistically analysed using 50 m as a stratification unit. The distribution of MRMR values in different stratifications of the east and west mining sections is shown in Figure 2. The MRMR values of each stratification range from 49 to 66.00, generally fluctuating around 57.5 with little variation. The MRMR values at the 1,050 m level in the east mining section and the 840 m level, as well as the 1,250 m and 1,400 m levels in the west mining section, are relatively lower and can be considered as the initial mining footprint.

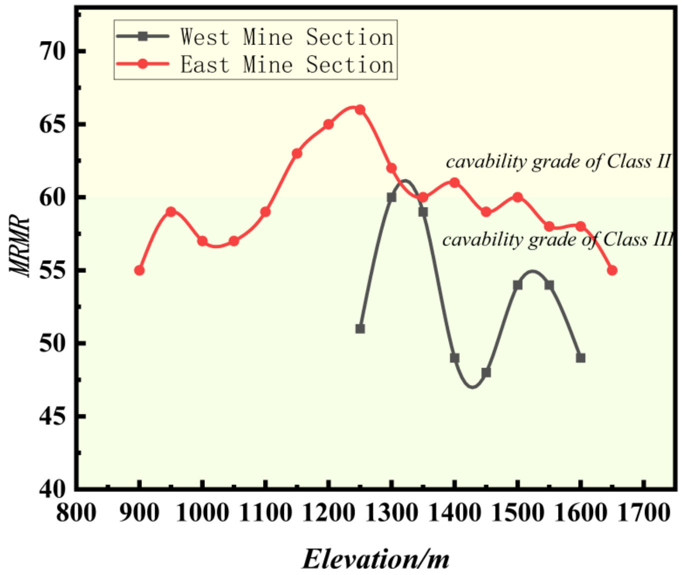

Figure 2 Distribution curves of mining rock mass rating values for different strata in the east and west mining sections

3.3 Prediction of caving areas

Based on the calculation results derived from the MRMR values, the hydraulic radii for the initial and continuous caving of the orebody were determined using the Laubscher caving diagram method (as shown in Figure 3). The hydraulic radius for continuous caving was determined using 2 distinct curves: curve A is applied when the aspect ratio of the orebody exceeds 1 ± 30%, and curve B is applied when the aspect ratio is less than 1 ± 30%.

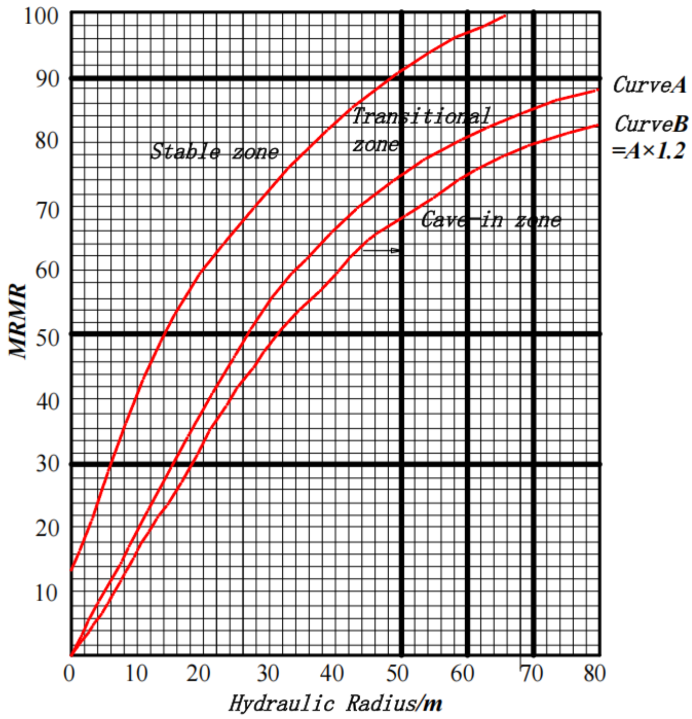

Figure 3 Laubscher's collapse diagram. MRMR = mining rock mass rating

Based on the above conditions for applying the Laubscher collapse diagram method, representative orebody lengths at different levels were measured at this gold mine, as shown in Table 3. It can be seen that curve A was selected for all orebodies within the Laubscher collapse diagram range at this gold mine.

Table 3 Selection of curves for the Laubscher collapse diagram method

Elevation (m)	Orebody length a (m)	Orebody width b (m)	a/b	Select curve
1,050	876	302	2.90	A
840	524	261	2.00	A
1,400	318	148	2.15	A
1,250	245	100	2.45	A

According to the statistical calculation results of MRMR, combined with the Laubscher collapse diagram method, the initial collapse hydraulic radius determined is between 13 and 25 m, as shown in Figure 4, with an initial collapse area of 2,922–10,394 m², averaging 5,000 m²; the sustained collapse hydraulic radius is between 26 and 39 m, with a sustained collapse area of 11,305–25,753 m², averaging 18,496 m², showing minor differences. In the MRMR evaluation, the eastern mine section at 840 and 1,050 m and the western mine section at 1,400 mm and 1,250 m are recommended as the initial mining levels, with relatively smaller initial collapse hydraulic radii in these intervals, making it relatively easier to achieve orebody collapse, and they can be considered as the initial mining levels.

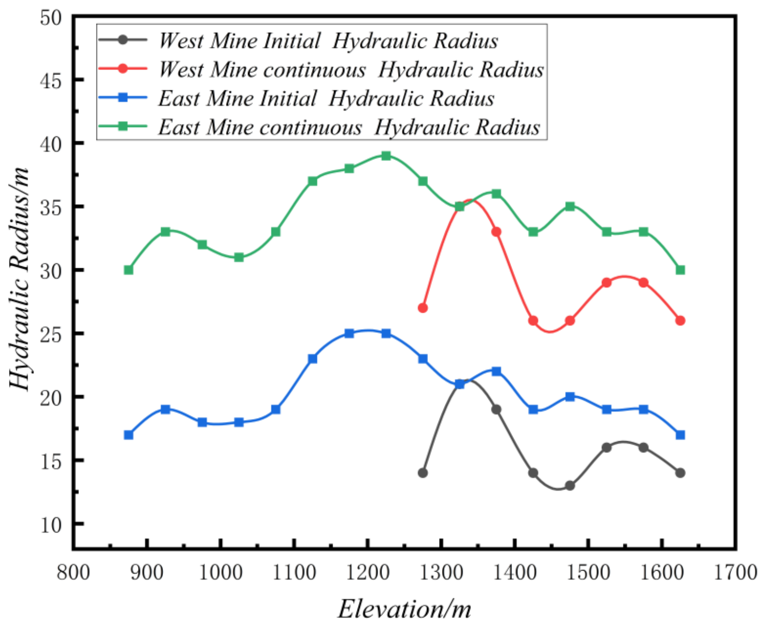

Figure 4 Distribution curves of initial and sustained hydraulic radii for different strata in the east and west mining sections

3.4 3D visualisation model development

Based on fundamental engineering geological parameters – including RQD ratings, joint spacing, structural plane conditions, groundwater conditions, rock strength, and joint orientation corrections – from a total of 99 boreholes in the borehole database, the MRMR statistical technique was used to evaluate the MRMR values for rock stability. Using 3DMine 3D numerical modelling software, a relatively accurate 3D visualisation model of rock mass quality was established based on existing data and information, as shown in Figure 5.

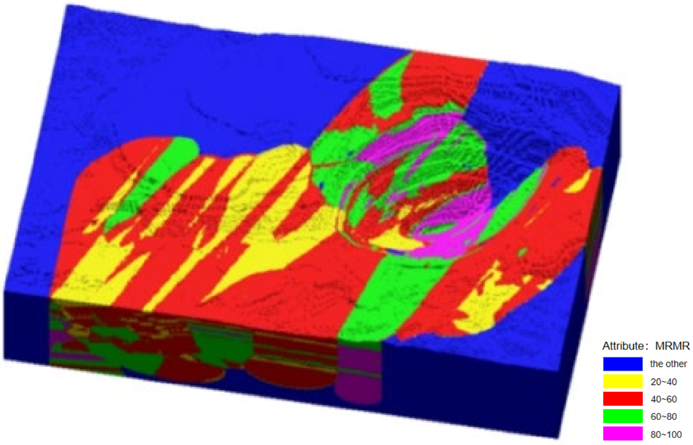

Figure 5 3D visualisation model of rock mass quality constructed using existing borehole data

Since the number of boreholes and their distribution do not cover the entire mining area, this paper introduces the KNN algorithm. The existing data from over 100 boreholes are used to predict MRMR values in unknown areas, thereby forming a three-dimensional MRMR evaluation model that covers the entire mining area.

In this paper, the data type for individual boreholes in the borehole database is defined as a 4-dimensional real-vector. The x and y coordinates of each borehole location are used as the x and y values of the data points, and the borehole depth is used as the z value. A three-dimensional Cartesian coordinate system is established to determine the position of each data point.

This paper uses Euclidean distance to calculate the distance between sample points. The formula is as follows:

$$d(x,y,z) = \sqrt{(x-x_i)^2 + (y-y_i)^2 + (z-z_i)^2} \quad (1)$$

In the equation, d(x, y, z) represents the distance between the borehole point to be predicted and a known borehole point; x, y, and z are the position coordinates of the borehole point to be predicted; and xi, yi, and zi are the position coordinates of the known borehole point.

Figure 6 shows a 3D visualisation model of rock mass quality and the statistical distribution of MRMR volume fractions, constructed using the prediction results of the KNN algorithm for unknown boreholes as indicators for the added virtual boreholes.

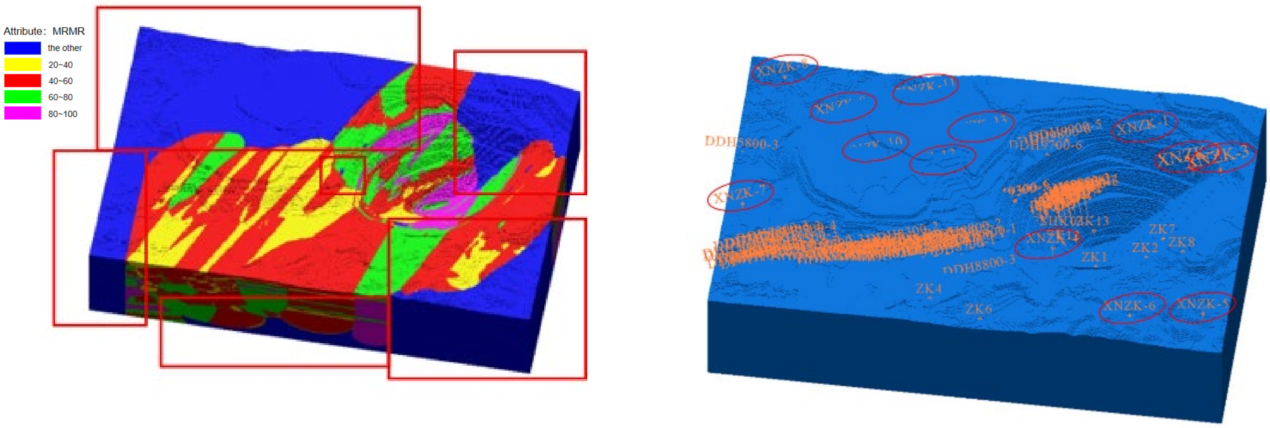

(a) (b)

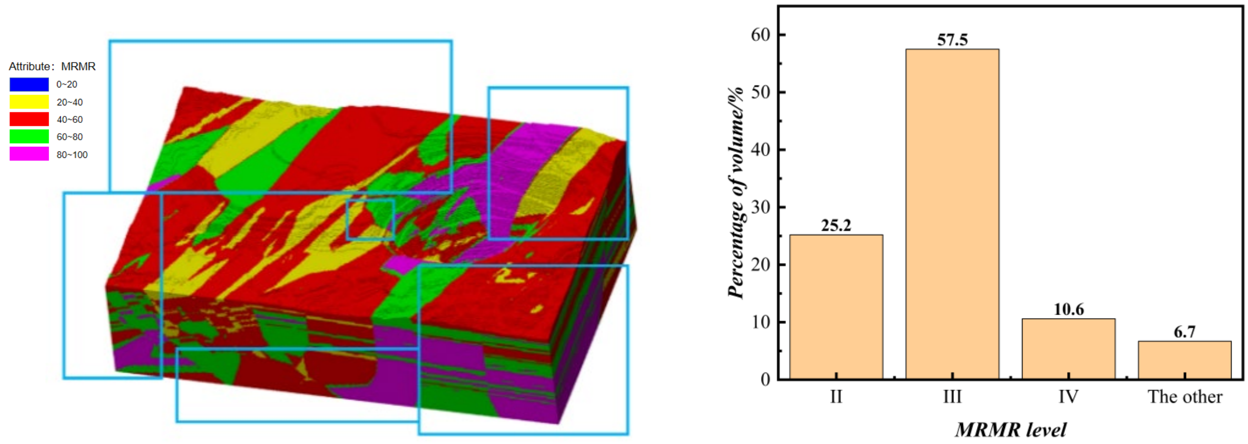

(c) (d)

Figure 6 3D visualisation model of rock mass quality derived from virtual geological borehole data using the K-nearest neighbour (KNN) algorithm. (a) Schematic diagram of the predicted area based on the KNN algorithm; (b) Distribution map of actual and virtual drilling holes; (c) The spatial distribution of mining rock mass rating (MRMR) values within the evaluation region after incorporating KNN data; (d) MRMR volume share chart

According to the caveability classification criteria, the 3D visualisation model of rock mass quality and the statistical diagram of volume proportions – both derived from virtual geological borehole data obtained using the KNN algorithm – show that the friability grades of this gold deposit within the overall evaluation area can be broadly divided into 3 categories: grade II, grade III, and grade IV. Among these, grade III friability zones account for the largest volume proportion, representing 57.5% of the total volume; grade II and grade IV friability zones account for 25.2 and 10.6% of the total volume, respectively. These friability grades correspond to 'difficult to break' and 'easy to break', respectively. Calculations show that the average MRMR value for the orebody in this mining area is 54, and the friability grade is comprehensively defined as grade III, indicating moderate friability.

4 BCF software for predicting caving fragmentation distribution

The fragmentation and size distribution of ore and rock in the block caving method are critical factors in caveability evaluation. The fragmentation of the ore is key to the success of the block caving method, as it affects various aspects including the orebody's caveability, the yield of large blocks, the flowability of the caved ore, the workload of secondary crushing, ore extraction methods and equipment selection, and the determination of the bottom structure. In this study, the BCF caving fragmentation software was used to analyse the initial fragmentation and the caving fragmentation in the study area.

4.1 Input of fragmentation prediction parameters

The geological parameters used for the caving fragmentation prediction analysis are shown in Figure 7a, while those for the 840 to 900 m section are shown in Figures 7b. It should be noted that all the analysis parameters listed here are derived from the analysis of field survey data and have been described in detail earlier in this paper; therefore, they will not be repeated here.

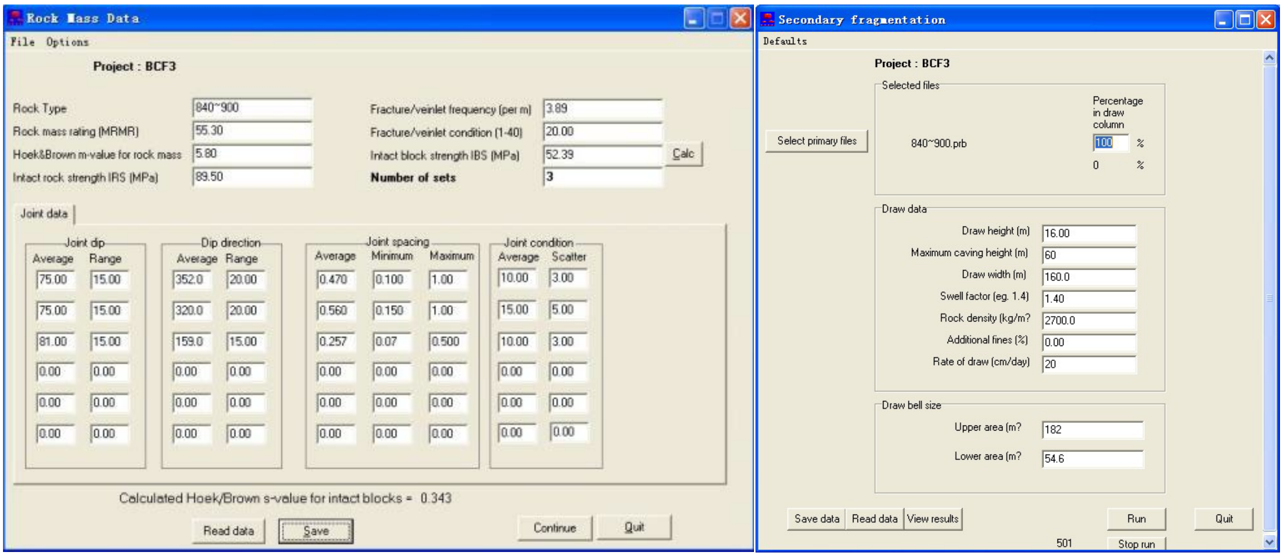

(a) (b)

Figure 7 Parameter input interface. (a) Geological parameter input; (b) Caving fragmentation parameter input

The average initial fragmentation prediction values are significantly different due to the different development of joints and fissures in different stratification sections, and the range of the initial caving fragmentation prediction values in different stratification sections is 0.44 to 1.67 m^3, as shown in Figure 8.

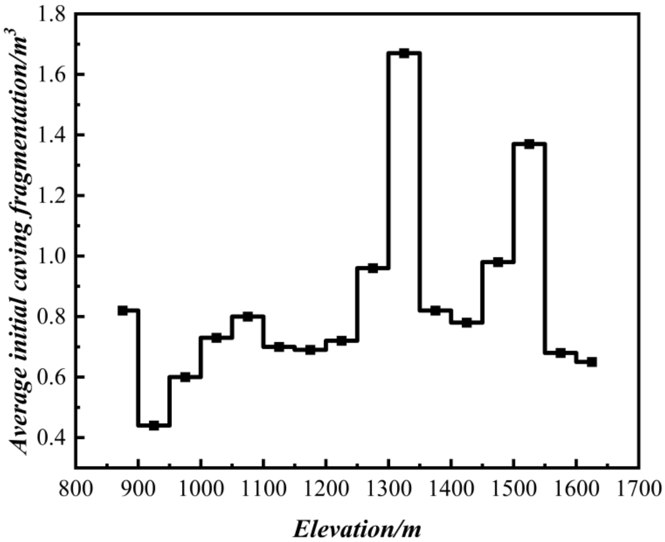

Figure 8 Distribution curves of average initial caving fragmentation by stratum (840–1,650 m levels)

4.2 Analysis of rockfall size prediction results

Within different sublevels, variations in joint and fracture development result in significant differences in the predicted average initial caving fragmentation. The predicted caving fragmentation shows little variation with stratification, as shown in Figure 9, where the predicted caving fragmentation within different strata ranges from 0.34 to 1.22 m^3.

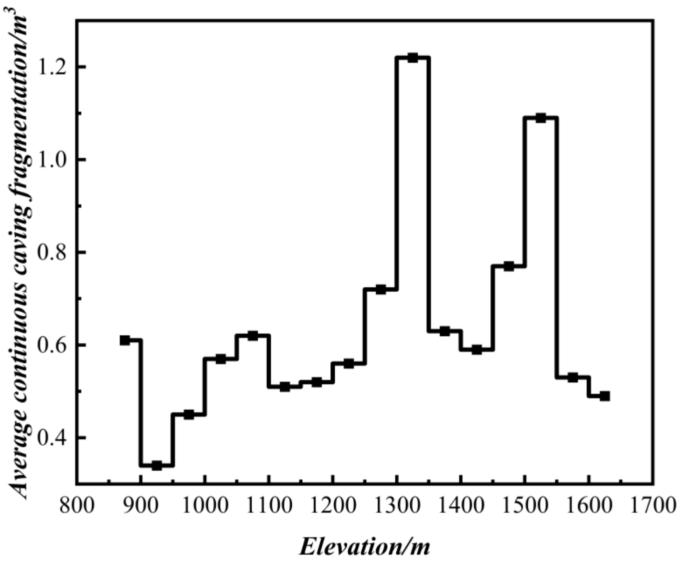

Figure 9 Distribution curves of average caving fragmentation by stratum (840–1,650 m elevation)

The analysis results of the initial fragmentation and caving fragmentation of the ore and rock at this mine using BCF software are within the range of the grade II–IV collapse requirement of the MRMR-based block caving evaluation standard, which shows that the calculated caving fragmentation of the mine meets the requirements of the caving fragmentation in the MRMR-based caveability evaluation standard, and it is verified that the caveability level of the gold mine in the overall evaluation area of the mine based on the KNN algorithm can be roughly divided into 3 levels, namely grade II, grade III and grade IV. The comprehensive definition of grade III is more accurate.

5 Numerical simulation of caveability

Because the ore and rock mass in this mining area is relatively fractured, numerical simulation of the surrounding rock collapse characteristics during the ore extraction process in this mine was conducted using the 3DEC 7.0 discrete element numerical simulation software. In this computational model, the initial in situ stress is assigned by writing a TXT text file, and the variation pattern of in situ stress with depth is shown in Figure 10.

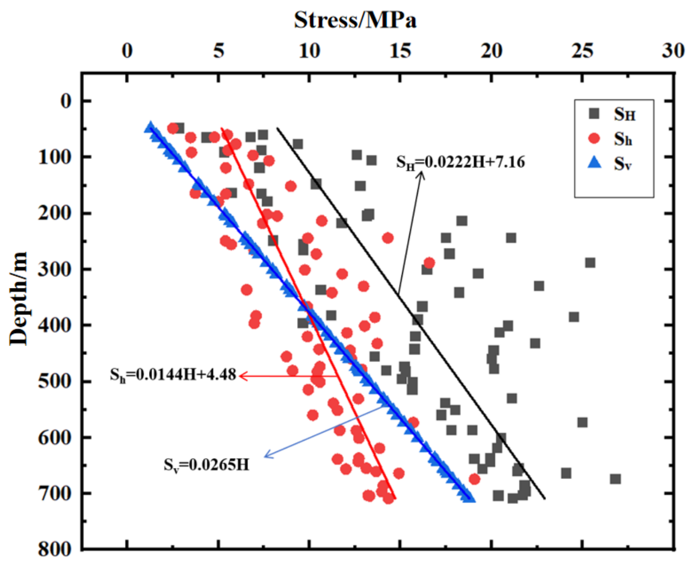

Figure 10 Variation pattern of in situ stress with depth

The model adopts the Mohr–Coulomb constitutive relationship. The physical and mechanical parameters of the rock blocks are listed in Table 4, and the physical and mechanical parameters of the joints are listed in Table 5. The boundary conditions are set as follows: displacement boundaries are applied to the left and right sides of the model, where the displacement of nodes in the X direction is constrained, while the Y and Z directions are free, forming a smooth contact surface. Similarly, displacement boundaries are applied to the front and back sides of the model, where the displacement of nodes in the Y direction is constrained, while the X and Z directions are free. The bottom of the model adopts a fixed boundary, where the displacements of nodes in the X, Y, and Z directions are all restricted to prevent any movement or rotation at the base. By applying the above boundary conditions and initial in situ stress field, the model is iteratively solved until it reaches overall equilibrium, and the initial in situ stress distribution of the rock mass is obtained. Subsequently, the initial displacement and velocity fields are reset to zero, and the equilibrated model is saved in .sav format to provide a basis for subsequent numerical simulations of the mining process.

Table 4 Physical and mechanical parameters of the rock blocks

Rock formations	γ (kN/m^3)	E_0 (GPa)	ν	ϕ (°)	C (MPa)	στ (MPa)
Biotite gneiss	27.1	7.33	0.23	38.49	2.81	2.15
Rhodendyl schist	28.0	10.97	0.23	38.15	2.06	3.43
Metamorphosed sandstone	28.6	6.17	0.24	38.69	2.51	2.17
Slate	28.1	5.01	0.27	36.23	1.57	1.01
Limestone	27.3	4.63	0.22	37.54	2.07	2.74

Table 5 Physical and mechanical parameters of the joints

Rock formations	Kn (GPa)	Ks (GPa)	ϕj (°)	Cj (MPa)	στj (MPa)
Biotite gneiss	10.5	3.3	28	0.50	0.3
Rhodendyl schist	8.1	2.5	26	0.4	0.2
Metamorphosed sandstone	7.6	2.7	30	0.7	0.3
Slate	5.2	1.5	25	0.3	0.15
Limestone	12.4	4	32	0.90	0.4

The simulation results are shown in Figure 11, and the rationality of the caveability evaluation results was verified using the 1,050 m ore extraction level in the east mine section as an example. The simulation results show that when the ore extraction area is 2,500 and 3,600 m^2, there is no subsidence or crack propagation. When it reaches 5,000 m^2, subsidence occurs at the centre of the ore extraction area, accompanied by crack propagation, indicating that the orebody begins to collapse at this point. When the ore extraction area reaches 20,000m^2, significant subsidence occurs near the centre of the ore extraction area, and continuous collapse starts. When the ore extraction area reaches 35,000–40,000m^2, significant subsidence and collapse occur near the centre of the ore extraction area, collapsing to the bottom. This pattern aligns with the predictions of the initial collapse area and the continuous collapse area in the collapse susceptibility evaluation, further demonstrating the feasibility of the collapse susceptibility evaluation results for this mine.

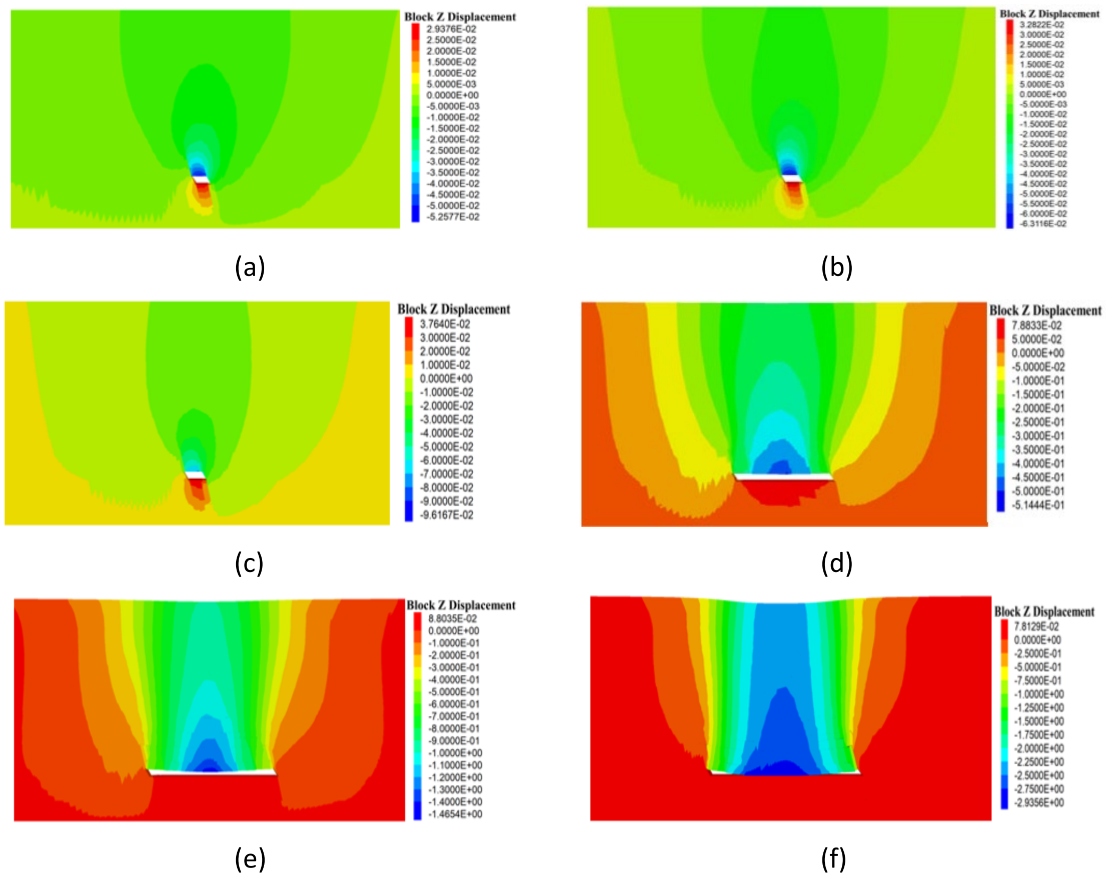

Figure 11 Collapse of ore and mine at different stages of the undercutting phase. (a) Collapse of the orebody at undercutting of 2,500 m^2; (b) Collapse of the orebody at undercutting of 3,600 m^2; (c) Collapse of the orebody at undercutting of 5,000 m^2; (d) Collapse of the orebody at undercutting of 20,000 m^2; (e) Collapse of the orebody at undercutting of 35,000 m^2; (f) Collapse of the orebody at undercutting of 40,000 m^2

6 Conclusion

Since there has been relatively little research on the natural caving method in China to date, and the limited studies that exist have focused on orebodies with relatively weak rock masses, the evaluation methods and results presented here – which apply to rock masses of relatively good quality – can provide valuable reference for the comprehensive evaluation of mine caving potential using the natural caving method under similar conditions in China. The main conclusions are as follows:

- According to the breakability evaluation criteria and MRMR statistical technique, by adopting a zonal evaluation method, the MRMR values of various stratified ore and rock between the 840 m level and surface of the east mining section and the 1,250 m level and surface of the west mining section were statistically analysed, with each 50 m as a stratification unit.
- Based on the preliminary determination of the collapse pattern using the Laubshcer collapse diagram, the initial and sustained collapse hydraulic radii of this mining area were initially determined to be 16 and 29 m, respectively. Correspondingly, the initial floor area required to reach mine production capacity in the east mining section is approximately 5,000 m^2, and the floor area required to achieve sustained collapse is approximately 18,946 m^2.
- Using the 3DMine software, a three-dimensional visualisation model for the MRMR rock mass quality evaluation was established based on the KNN algorithm to obtain virtual geological drilling data. The statistics show that the breakability grade of the gold mine in the overall evaluation area

can be roughly divided into class II, class III, and class IV. The average value is calculated to be 54, and the comprehensive evaluation is defined as class III, medium breakability.

- Using the BCF software, the collapse caving fragmentation of this mining area is predicted to be within the range of 0.34 to 1.22 m^3, which meets the class III, medium breakability standard, verifying the breakability evaluation grade.
- The numerical analysis method simulated the ore extraction process in the block caving area of the gold mine. The simulation showed that when the initial caving area reached about 5,000 m^2, the initial caving level area began to extract ore, and when the caving area reached 20,000 m^2, continuous caving was achieved, verifying the rationality of the caving potential evaluation and the prediction results of the initial caving area.

Acknowledgement

The authors gratefully acknowledge the financial support from the National Key Research and Development Program of the Deep Earth Science Funded Project (Grant No. 2024ZD1003806), and acknowledges the Caving 2026 conference for providing this excellent platform and for all those who helped and supported the writing of this paper, especially Professor Cao Hui and Senior Engineer Xie Lianku of the Information Research Institute of the Ministry of Emergency Management for their guidance on my thesis.

Use of artificial intelligence disclosure statement

In the preparation of this work, the authors used DeepSeek to improve the language and clarity of their writing. The authors have reviewed the content and edited it where required and take full responsibility for said content.

References

Cao, H, Yu, SB, Wang, H, Qin, XS & Yuan, Y 2016, 'Comprehensive evaluation of block caving feasibility based on MRMR', *Chinese Journal of Rock Mechanics and Engineering*, vol. 35, no. S2, pp. 4148–4153.

Feng, XL, Wang, LG, Bi, L, Jia, MT & Zeng, QT 2008, 'Study on ore-body cavability based on Laubscher caving chart', *Journal of China Coal Society*, vol. 33, no. 3, pp. 268-272.

Laubscher, DH 1994, 'Cave mining the state of the art', Journal of South African Institute of Mining and Metallurgy, vol. 94, no. 10, pp. 279–293.

Liu, H & He, RX 2024, *Research and Application of Rock Mass Caveability Evaluation System for Block Caving*, Metallurgical Industry Press, Beijing.

Mariager, S & Fargher, M 2024, 'Loop de Loop – An innovative block cave extraction level design for BC1 at Carrapateena', in D Johansson & H Schunnesson (eds), *MassMin 2024: Proceedings of the International Conference & Exhibition on Mass Mining*, Luleå University of Technology, Luleå, pp. 17–31, https://doi.org/10.36487/ACG_repo/2435_A-02

Tong, JH 2025, 'Study on fragmentation prediction and distribution law of block caving mine in kilometer-deep well', Gold, vol. 46, no. 2, pp. 13-17.

Wang, LC, Shao, AL, Qu, FM, Yue, XT, Wang, HY, Zhang, XF & Liu, XB 2025, 'Current status and prospects of metal mining technology', *Chinese Journal of Engineering*, vol. 47, no. 5, pp. 971–983.

Wang, YC, Wang, K, Wang, JH & Qin, XS 2023, 'Cavability evaluation and caving evolution law of ore rock in Tongshan Mine', *Nonferrous Metals Engineering*, vol. 13, no. 6, pp. 89–97.

Wu, AX, Wang, Y, Zhang, MZ & Yang, GF 2021, 'New progress and prospect of key technologies for underground mining in metal mines', *Metal Mine*, vol. 50, no. 1, pp. 1–13.

Zhang, Q & Hocking, RJ 2022, 'Carrapateena block cave mine design and planning: feasibility study', in Y Potvin (ed.), *Caving 2022: Proceedings of the Fifth International Conference on Block and Sublevel Caving*, Australian Centre for Geomechanics, Perth, pp. 291–302, https://doi.org/10.36487/ACG_repo/2205_19